

Micromachined Sensors Using Polysilicon Sacrificial Layer Etching Technology

Osamu Tabata, Keiichi Shimaoka, Ryouji Asahi and Susumu Sugiyama¹

Toyota Central Research & Development Laboratories, Inc.
Nagakute-cho, Aichi-gun, Aichi 480-11, Japan
¹Department of Mechanical Engineering,
Ritsumeikan University
Noji-cho, Kusatsu, Shiga 525-77, Japan

(Received October 20, 1995; accepted November 6, 1995)

Key words: silicon sensor, micromachined sensor, integrated sensor, polysilicon, sacrificial layer etching, pressure sensor, infrared sensor, optical chopper, actuator, preassembly

Polysilicon sacrificial layer etching technology is presented as one of the key sensor assembly technologies to improve the cost performance of silicon sensors. Its application in a microdiaphragm pressure sensor with a reference pressure chamber and an integrated pyroelectric infrared sensor with a thermal isolated structure is demonstrated. Fabrication of a micro-optical chopper is shown, and the future of sensor devices is considered.

1. Introduction

In many industrial fields, including the automobile industry, sensors are occupying an increasingly important position as key devices which determine system performance. At the same time, sensors themselves are required to have high performance. Silicon micromachined sensors are extremely promising as sensors which meet this requirement.

In this paper, we focus on silicon micromachined sensors. First, the trend of silicon sensor integration is reviewed. Second, polysilicon sacrificial layer etching technology, which is one of the promising sensor fabrication technologies, and its applications in a microdiaphragm pressure sensor and a pyroelectric infrared sensor are presented. Finally, fabrication of a micro-optical chopper for pyroelectric infrared sensors is proposed, and the future of silicon sensor devices is considered.

2. Silicon Sensor Integration Trend

The trend in silicon sensor integration is said to be advancing in the following steps.

Phase 1: Sensor (discrete).

Phase 2: Sensor + IC.

Phase 3: Sensor + IC + Microprocessor.

The present stage is phase 2. As an example of the contribution of the progress of silicon sensor integration to the improvement of sensor cost performance in phase 2, our research and development of silicon sensors is expressed and evaluated using

$$\text{Cost performance} = FT / (ARC),$$

where F is the pressure range (Pa), T is the compensated temperature range ($^{\circ}\text{C}$), A is the accuracy (%F.S.), R is the resolution (Pa) and C is total cost of fabrication (¥). The total cost includes the cost of the peripheral circuits required for obtaining the temperature-compensated output of a voltage level, and its adjustment and assembly costs.

Figure 1 shows the progress in research and development of integrated silicon pressure sensors. A practical piezoresistive pressure sensor was first presented in 1973.⁽¹⁾ Four piezoresistors connected to each other via a bridge circuit were formed on a silicon chip, and the output obtained was 50–100 mV. At that time, the cost performance was 100. In 1983, amplifiers were integrated, and therefore output increased to the voltage level.⁽²⁾ The cost performance became 200 due to cost reduction by integration. However, the output and temperature characteristics had to be adjusted and compensated on external circuits. In 1989, peripheral circuits, such as amplifiers and thin film trimming resistors, were inte-

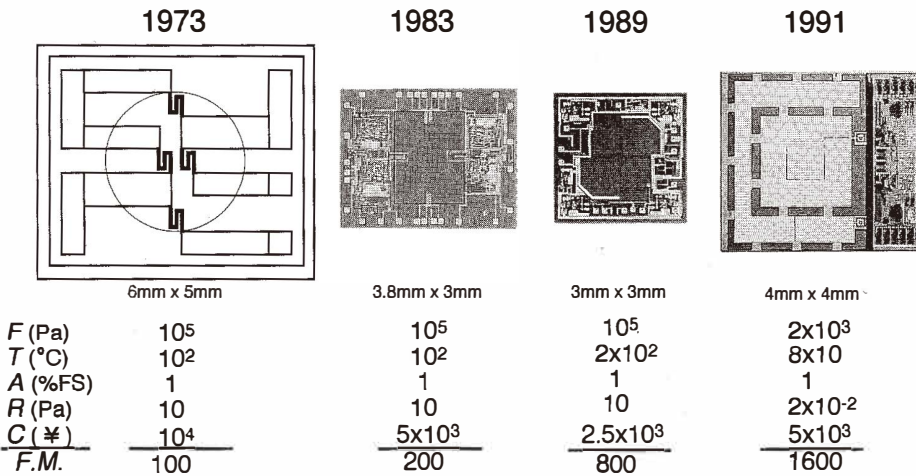


Fig. 1. Progress in research and development of integrated silicon pressure sensor.

grated in the pressure sensor, and the compensated temperature range was then extended and the adjustment cost was reduced.⁽³⁾ Therefore, the cost performance was raised to 800. In 1991, the detection principle was changed from a piezoresistive type to a capacitive type, and a sensor integrated with digital processing circuits that has high sensitivity and resolution in a pressure range of 2 kPa was realized.⁽⁴⁾ This improvement of resolution rapidly raised the cost performance to 1600.

The figure of merit can be defined as the relative ratio of the cost performance of integrated silicon pressure sensors to the cost performance of the pressure sensors developed in 1973, and is plotted for each year, as shown in Fig. 2. In 1983, sensors were integrated with amplifiers and the figure of merit was 2. In 1989, sensors were integrated with peripheral circuits and the figure of merit was 8. In 1991, capacitive-type sensors were integrated with digital processing circuits and the figure of merit became 16. The trend in the figure of merit shows a linear increase illustrated by the solid line in Fig. 2.

As for the integrated silicon sensor itself, the cost performance has been rapidly raised to a high level. One of the key technologies in improving the figure of merit in the future is sensor assembly technology including packaging because the sensor assembly cost now accounts for the majority of total sensor cost. As a new approach towards reducing the total sensor cost, micromachined sensors are introduced. The main feature of the micromachined sensors is that they can be automatically formed without any complicated assembly process such as the glass bonding process, thus effectively reducing the sensor assembly cost. As an example, a microdiaphragm pressure sensor⁽⁵⁾ is described here.

Next, phase 3 is reviewed. With the present level of technology, "Sensor + IC + Microprocessor" can be produced. However, there is almost no example of its practical

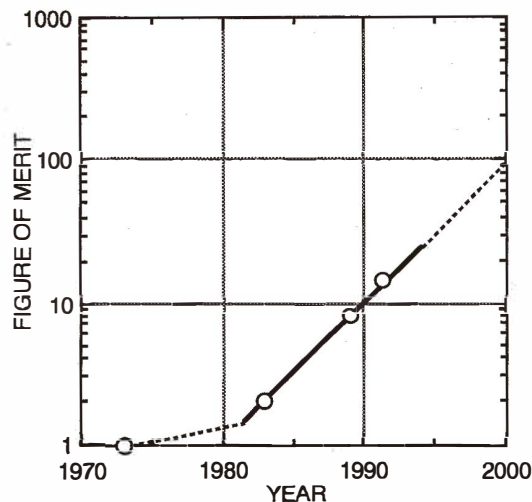


Fig. 2. Trend in figure of merit of integrated silicon pressure sensor.

application as yet. This is because the integration of a microprocessor with a sensor does not immediately contribute to the improvement of the figure of merit of the silicon sensor itself. This is clear from the definition of the figure of merit mentioned above. In the future, when a common standard of the sensor bus becomes established and sensors become capable of communicating with each other,⁽⁶⁾ the integration of a microprocessor with a sensor is expected to advance.

We interpret that phase 3 of silicon sensor integration means the organization of "Sensor + IC + Actuator," such as the servo accelerometer presented by Analog Devices Inc.⁽⁷⁾ The servo system and self-calibration will certainly contribute to a dramatic rise in the figure of merit through improvements in the dynamic range, accuracy, resolution and assembly process.⁽⁸⁾ As examples of this approach, an integrated infrared sensing system consisting of a pyroelectric infrared sensor⁽⁹⁾ and a micro-optical chopper⁽¹⁰⁾ will be presented.

3. Polysilicon Sacrificial Layer Etching

Sacrificial layer etching technology involves a sacrificial layer, a movable structure layer, a passivation layer that protects the integrated circuit, and an etching solution. Polysilicon sacrificial layer etching technology is generally used in the fabrication of integrated sensors. When polysilicon is used for the sacrificial layer, the following materials may be used: polysilicon and silicon nitride for the structure layer, silicon nitride for the passivation layer, and most anisotropic etchants such as KOH, ethylene diamine pyrocatechol (EDP), hydrazine and tetramethyl ammonium hydroxide (TMAH). Deep grooves can be formed by combining polysilicon sacrificial layer etching with silicon substrate anisotropic etching.⁽¹¹⁾

Polysilicon heavily doped with boron shows an etch-stop characteristic similar to that of single-crystal silicon. Figure 3 shows the dependence of relative etch rate on boron concentration for the polysilicon layer. When polysilicon is doped with boron to a concentration of $4 \times 10^{20} \text{ cm}^{-3}$, the relative etch rate of 10^{-2} is obtained in a solution of TMAH with a concentration equal to or below 20 wt.%.⁽¹²⁾ Therefore, the etch-stop characteristic of polysilicon is practical.

Applying these features of polysilicon sacrificial layer etching, microstructures of any shape can be accurately fabricated on a silicon substrate, as shown in Fig. 4: microcavities, movable membranes, flow channels, diaphragms and thermally isolated structures. Therefore, realization of high-performance microsensors and microactuators is guaranteed.

4. Microdiaphragm Pressure Sensor

Since our presentation of the first microdiaphragm pressure sensor fabricated by surface micromachining at IEDM in Los Angeles in 1986,⁽¹³⁾ microdiaphragm pressure sensors have been continuously improved for practical use. In this section, a practical microdiaphragm pressure sensor fabricated by polysilicon sacrificial layer etching is

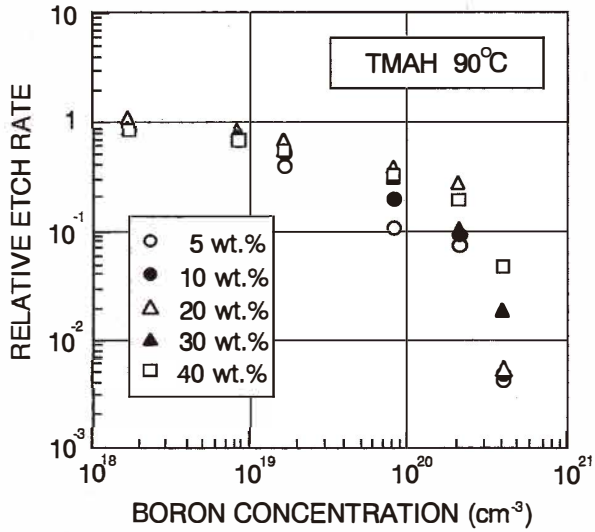


Fig. 3. Dependence of relative etch rate on boron concentration for polysilicon layer.

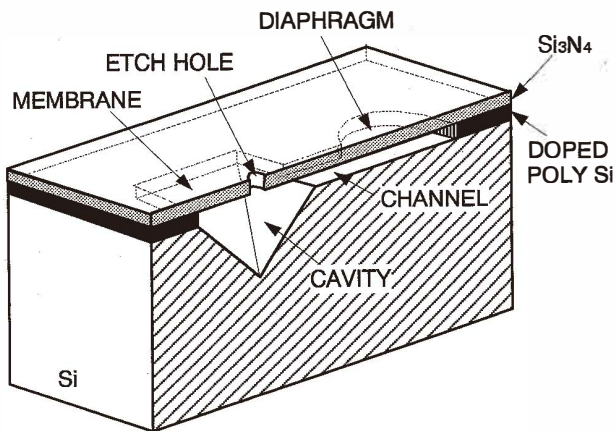


Fig. 4. Schematic diagram of microstructure fabricated using polysilicon sacrificial layer etching technology.

presented.⁽⁵⁾

Figure 5 shows the schematic cross-sectional structure of the microdiaphragm pressure sensor. Four polysilicon piezoresistors with a width of $2\ \mu\text{m}$ are formed on a silicon nitride diaphragm with a diameter of $100\ \mu\text{m}$. Polysilicon sacrificial layer etching progresses radially from the central etch hole of $10\ \mu\text{m}$ diameter in the diaphragm and automatically stops at the border of the boron-doped region of the shape designed in advance. A circular diaphragm is used to reduce the stress concentration to avoid diaphragm fracture during the etching process. The central etch hole is sealed with plasma chemical vapor deposition (CVD) silicon nitride and silicon dioxide at the end of the fabrication process. The final thickness of the diaphragm is $1.7\ \mu\text{m}$. This results in a diaphragm production yield of more than 99%. The pressure sensitivity and temperature characteristics of the pressure sensor depend on the values and distribution of mechanical properties such as the internal stress and Young's modulus of a composite membrane such as a pressure diaphragm consisting of silicon nitride and silicon dioxide. Therefore, CVD processes must be carried out under optimum conditions.⁽¹⁴⁾ A scanning electron microscope (SEM) image of the microdiaphragm is shown in Fig. 6. Characteristics of the pressure sensor are summarized in Table 1.

The advantages of the microdiaphragm pressure sensor are its ultraminiature size, and that it is of a preassembly type so that a reference pressure chamber can be formed without an extra assembly process such as glass bonding that is conventionally required. The proposed preassembled pressure sensor ensures ultraminiature size and low cost for a wide range of applications.

5. Integrated Infrared Sensor

The use of thermal infrared sensors without a cryogenic cooler is advantageous for miniaturization and cost reduction of the sensing system in a wide range of applications including automobiles. In order to increase the sensitivity and response of thermal infrared sensors, sensing elements must be thermally isolated from the substrate. By polysilicon

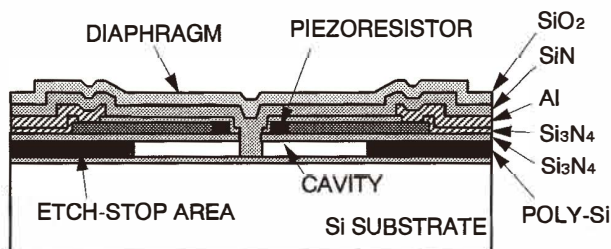


Fig. 5. Cross-sectional structure of the microdiaphragm pressure sensor fabricated using polysilicon sacrificial layer etching technology.

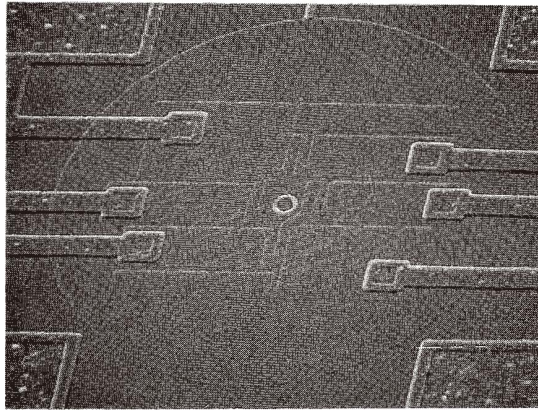


Fig. 6. SEM micrograph of the microdiaphragm.

Table 1
Characteristics of the microdiaphragm pressure sensor.

Supply voltage (V)	3
Pressure range (abs.) (kPa)	60 to 110
Sensitivity ($\mu\text{V}/\text{V}/\text{kPa}$)	20
Nonlinearity (%F.S.)	<1
Temperature range ($^{\circ}\text{C}$)	-30 to 85
Sensitivity temperature coefficient ($\%/^{\circ}\text{C}$)	-0.26
Resonant frequency (MHz)	20

sacrificial layer etching, membranes can be kept afloat from the substrate, leading to the formation of an excellent thermally isolated structure. An integrated infrared imaging sensor using a polysilicon p-n junction has been fabricated, and the effectiveness of the thermally isolated structure formed by polysilicon sacrificial layer etching has been confirmed.⁽¹⁵⁾

5.1 Integrated pyroelectric infrared sensor

Figure 7 shows the schematic cross-sectional structure of the thermal integrated infrared sensor with a polyvinylidene fluoride (PVDF) pyroelectric detecting element.⁽⁹⁾ Figure 8 is a micrograph of the fabricated infrared sensor chip before formation of an absorbent. The infrared sensor was fabricated by anisotropic etching combined with polysilicon sacrificial layer etching. The sensor element with a sensing area of $400 \times 400 \mu\text{m}^2$ and metal oxide semiconductor field effect transistors (MOSFETs) are integrated on a silicon substrate. In order to reduce the thermal capacitance of the sensor element and the

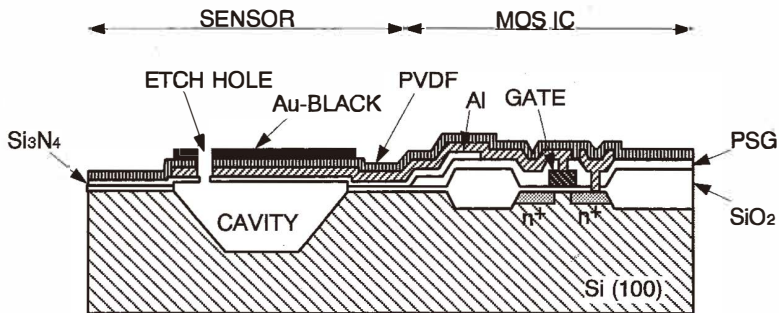


Fig. 7. Cross-sectional structure of the thermal integrated infrared sensor with a PVDF pyroelectric detecting element.

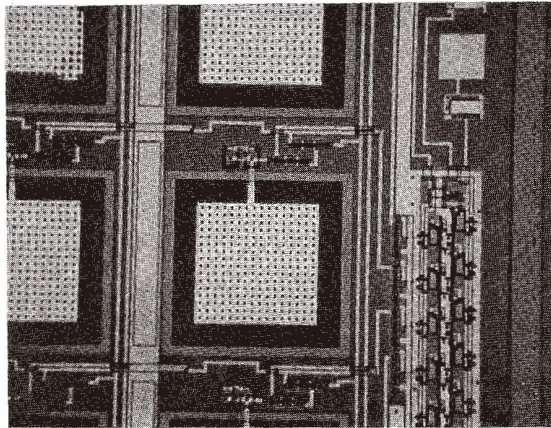


Fig. 8. Micrograph of the fabricated infrared sensor chip before formation of an absorbent.

thermal conduction from the sensor element to the substrate, the sensor element is equipped with a membrane structure supported by Si₃N₄ with a thickness of 150 nm. A number of etch holes with a diameter of 10 μm are formed in the membrane. These holes are necessary for uniform etching under the sensor area, as well as for reducing the thermal capacitance and conduction of the membrane. A PVDF film is formed on the Al lower electrode on the membrane by an electrospray method.⁽⁹⁾ Typical thickness of the PVDF is 1–2 μm. The upper electrode, Au-black, which functions as an absorbent of infrared rays, is formed on top of the sensor element. The output signals are impedance-transferred and led to external electronics by on-chip MOSFETs.

The characteristics of the infrared sensor are summarized in Table 2. The features of

Table 2
Characteristics of the pyroelectric infrared sensor.

Sensing area (μm^2)	400 × 400
PVDF thickness (μm)	2
Pyroelectric coefficient ($\text{nCcm}^{-2}\text{K}^{-1}$)	2 – 4
Responsivity (V/W)	125 (10 Hz)
Detectivity ($\text{cmHz}^{1/2}\text{W}^{-1}$)	1.4×10^7 (500,100,1)
NEP ($\text{Hz}^{-1/2}\text{W}$)	2.9×10^{-9} (500,100,1)
Thermal time constant (ms)	1.3

the sensor, including the structure and the fabrication technology, are highly advantageous to the performance, productivity and realization of an on-chip two-dimensional infrared imager.

5.2 Micro-optical chopper

Pyroelectric infrared sensors detect only the temperature change ΔT caused by incident infrared rays. Therefore, it is necessary to use an optical chopper for operation of the pyroelectric infrared sensor to detect differences of the temperature between the object and a reference. A magnetic motor with a chopping wheel is conventionally used for operation of the pyroelectric infrared sensor. In order to reduce the size of the infrared sensing system and production cost, the optical chopper must be miniaturized and the chopper assembly process improved.

Figure 9 shows a SEM micrograph of the micro-optical chopper fabricated using a

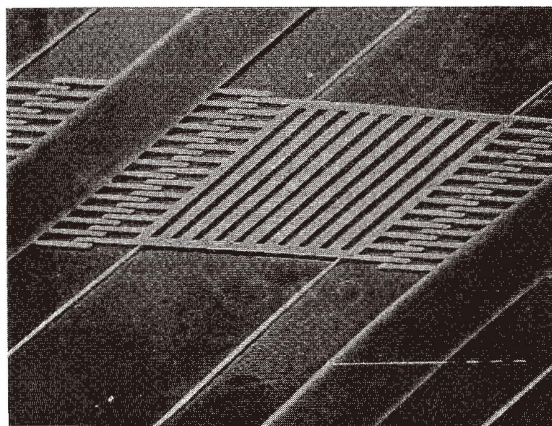


Fig. 9. SEM micrograph of the micro-optical chopper.

combination of silicon dioxide sacrificial layer etching and silicon anisotropic etching.⁽¹⁰⁾ In the fabrication process of the optical chopper, a silicon-on-insulator (SOI) wafer is used as the starting material. High reliability can be expected because of the well-defined mechanical properties of single-crystal silicon. The principle of the optical chopper is based on an electrostatic comb-drive actuator with two doubly supported beams. The moving slits are electrostatically driven by comb electrodes arranged on their two sides. An aluminum layer is deposited as a reflector on the slit frames and the silicon substrate. When the slits are at their original positions infrared rays are reflected by the aluminum reflector. When the slits deviate from their original positions, infrared rays pass through the slits and silicon substrate. The silicon substrate acts as an infrared filter to cut off wavelengths below $1 \mu\text{m}$.

Figure 10 shows the concept of the integrated infrared sensing system which combines an infrared sensor and the micro-optical chopper. The optical chopper chip is stacked on the infrared sensor chip in a wafer state. The individual slits are aligned with corresponding sensor elements on the chip. The micro-optical chopper can be operated under the optimum conditions for obtaining the maximum sensitivity of the sensor element. The concept proposed here is an excellent example of phase 3 application and is expected to improve the sensor performance without the need for a complicated optical chopper or an expensive assembly process.

6. Conclusions

First, the trend in silicon sensor technology was reviewed, and sensor assembly was shown to be a key technology in improving the sensor cost performance. Second, to achieve the improvement of the sensor cost performance, polysilicon sacrificial layer

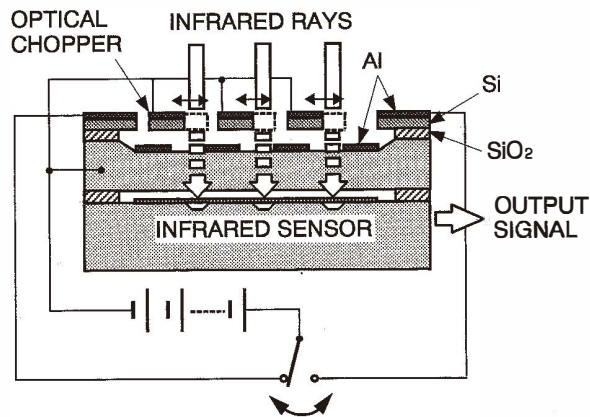


Fig. 10. Integrated infrared sensing system with a micro-optical chopper.

etching technology and its applications to the fabrication of sensors were presented. Finally, a micro-optical chopper was shown, and the future of sensor devices was considered. We interpreted that the final step of silicon sensor integration, phase 3, means the organization of "Sensor + IC + Actuator," which will lead to a dramatic rise in the figure of merit, through improvements of the dynamic range, accuracy, resolution and assembly process. The above approach will provide the sensor technology to enable us to reach our final goal of "System on a microchip," and contribute to progress in the fields of electronics, mechanics, bionics and medicine.

References

- 1 S. Sugiyama, H. Nakamura, K. Hayakawa and I. Igarashi: Abstracts of the 20th Conf. of Japan Soc. of Appl. Phys., March (1973) p.148 (in Japanese).
- 2 S. Sugiyama, M. Takigawa and I. Igarashi: *Sensors and Actuators* **4** (1983) 63.
- 3 S. Yamashita, K. Shimaoka, H. Funahashi, S. Sugiyama and I. Igarashi: Technical Dig. of the 8th Sensor Symposium, Tokyo (1989) p.13.
- 4 T. Nagata, H. Terabe, S. Kuwahara, S. Sakurai, O. Tabata, S. Sugiyama and M. Esashi: *Sensors and Actuators* **A34** (1991) 173.
- 5 K. Shimaoka, O. Tabata, M. Kimura and S. Sugiyama: Proc. of Transducers '93, Yokohama (1993) p.632.
- 6 K. D. Wise and N. Hajafi: Proc. of Transducers '91, San Francisco (1991) p.2.
- 7 R. S. Payne and K. A. Dinsmore: SAE paper, Detroit (1991) p.127.
- 8 F. Pourahmadi, L. Christel and K. Petersen: Tech. Dig. of the IEEE Solid-State Sensor and Actuator Workshop (1992) p.122.
- 9 R. Asahi, J. Sakata, O. Tabata, M. Mochizuki, S. Sugiyama and Y. Taga: Proc. of Transducers '93, Yokohama (1993) p.1656.
- 10 O. Tabata, R. Asahi, N. Fujituka, M. Kimura and S. Sugiyama: Proc. of Transducers '93, Yokohama (1993) p.124.
- 11 O. Tabata, H. Funabashi, K. Shimaoka, R. Asahi and S. Sugiyama: Proc. of the 2nd International Symposium on Micro Machine and Human Science, Nagoya (1991) p.163.
- 12 K. Shimaoka, O. Tabata and S. Sugiyama: Tech. Dig. of the 10th Sensor Symposium, Tokyo (1991) p.25.
- 13 S. Sugiyama, T. Suzuki, K. Kawahata, K. Shimaoka, M. Takigawa and I. Igarashi: Tech. Dig. of IEDM '86, Los Angeles (1986) p.184.
- 14 K. Shimaoka, O. Tabata, S. Sugiyama and M. Takeuchi: Tech. Dig. of the 12th Sensor Symposium, Osaka (1994) p.27.
- 15 R. Asahi, O. Tabata, F. Suzuki, S. Sugiyama, M. Suzuki and A. Tanaka: Tech. Dig. of the 11th Sensor Symposium, Tokyo (1992) p.99.